Article

Journal of
Biomedical Nanotechnology
Vol. 16, 1–9, 2019
www.aspbs.com/jbn

MXene Nanosheets May Induce Toxic Effect on the Early Stage of Embryogenesis

Hashim Alhussain[1, †], Robin Augustine[1, 2, †], Essraa A. Hussein[3], Ishita Gupta[4], Anwarul Hasan[1, 2], Ala-Eddin Al Moustafa[1, 4, *], and Ahmed Elzatahry[5, *]

[1] *Biomedical Research Center, Qatar University, Doha, Qatar*
[2] *Department of Mechanical & Industrial Engineering, College of Engineering, Qatar University, Doha, Qatar*
[3] *Material Science and Technology Program, College of Arts & Science, Qatar University, Doha, Qatar*
[4] *College of Medicine, QU Health, Qatar University, Doha, Qatar*

MXene ($Ti_3C_2T_x$), as a novel 2D material, has produced a great interest due to its promising properties in biomedical applications, nevertheless, there is a lack of studies dedicated to investigate the possible toxic effect of MXene in embryos. Herein, we aim to scrutinize the potential toxicity of MXene nanosheets on the early stage of the embryo as well as angiogenesis. Avian embryos at 3 and 5 days of incubation were used as an experimental model in this investigation. Our findings reveal that MXene may produce adverse effect on the early stage of embryogenesis as ~46% of MXene-exposed embryos died during 1–5 days after exposure. We also found that MXene at tested concentration inhibits angiogenesis of the chorioallantoic membrane of the embryo after 5 days of incubation. More significantly, RT-PCR analysis of seven genes, which are key regulators of cell proliferation, survival, cell death and angiogenesis, revealed that these genes were deregulated in brain, heart and liver tissues from MXene-treated embryos in comparison with their matched controls. Our study clearly suggests that MXene at studied concentration might induce a toxic effect on the early stage of embryogenesis; nevertheless, more investigations are necessary to understand the effect at low concentrations and elucidate its mechanism at the early stage of normal development.

KEYWORDS: *MXene, $Ti_3C_2T_x$, Avian Embryo, Angiogenesis, Toxicity, Gene Expression.*

INTRODUCTION

In recent years, many nanomaterials such as metallic nanoparticles [1, 2], metal oxide nanoparticles [3], carbon nanostructures [4, 5] and polymeric nanoparticles [6] have been widely used in many fields. MXenes are a novel family of 2D materials which have shown a great potential in a myriad of industrial and biomedical applications. Due to their ultrathin planar structure, MXenes exhibit promising physiochemical properties with great application potentials in the biomedical field [7, 8]. MXene ($Ti_3C_2T_x$) was discovered in 2011 as a 2D ceramic material made of bulk crystal called MAX [9], where in MAX phase, "M" represents an early transition metal (e.g., titanium), "A" represents the IIIA or IVA group elements, and "X" is either carbides (C) or nitrides (N). MXenes have a general formula of $M_{n+1}X_nT_x$ [10]. As known, the M–X covalent bonds and M–A metallic bonds in the MAX phase are quite strong. However, by utilizing robust etchants (hydrofluoric acid or lithium fluoride-hydrochloric acid mixtures [11] or ammonium hydrogen bifluoride [12, 13], the reactive M–A bonds can be destroyed and the A-element layers can be selectively detached, resulting in multilayered (m-) MXene with a general formula $M_{n+1}X_nT_x$ ($n = 1, 2, 3$), where T_x are surface-termination functionalities [14]. Since it involves carbides and/or nitrides, MXene inherently has good conductivity, which makes it a great candidate for next-generation energy storage devices [15]. Additionally, due to its versatile chemistry, MXene ($Ti_3C_2T_x$) has shown potential in a wide range of applications including purifying water, chemical sensors, photo- or electro catalysis, electromagnetic interference shielding, and many applications in the biomedical field including drug

*Authors to whom correspondence should be addressed.
Emails: aalmoustafa@qu.edu.qa, aelzatahry@qu.edu.qa
†These two authors contributed equally to this work.
Received: 17 January 2020
Accepted: 19 March 2020

delivery as well as molecular imaging [16–19]. MXene nanosheets can serve as drug carriers; with its high specific surface area that can accommodate abundant anchoring sites and reservoirs as well [20]. The ultrathin structure also contributes to various possible biological applications such as enzyme-triggered biodegradation, cellular endocytosis, distinct biodistribution, and metabolism pathways [20–23]. Moreover, the ability of tailoring the structure of MXene to precise design synthesized in the pristine structure of MAX phase, contributes to the flexible and extensive multi-functionalities of MXenes, and creates promising potential for theranostic nanomedicine [24].

A few studies investigated the effect of MXene *in vitro* and *in vivo* [25, 26]. In this context, different cell line models were used to investigate the cytotoxicity of MXene [22], these studies demonstrated that MXene has low cytotoxicity to normal cells and higher toxic effect against cancerous cells [22, 25, 26]. Although such results might seem promising, *in vitro* results do not always correlate well with *in vivo* counterparts. While, a limited number of studies regarding the outcome of MXene *in vivo* were performed, few of these studies suggest minor toxic effect on animal models [27]. More specifically, a recent study, using zebrafish, evaluated the biocompatibility of MXene on oral tissue and body weight screening, their results did not show a significant toxic effect of MXene [27]. Nevertheless, due to complete lack of information on the outcome of MXenes on vertebrate embryogenesis and angiogenesis. Herein, we explored the outcome of MXene ($Ti_3C_2T_x$) on the early stage of the normal development and angiogenesis using the chicken embryo and its chorioallantoic membrane (CAM as a model), which is largely used by our group [28]. Our study pointed out, for the first time, that MXene provokes a significant toxic effect on the embryo; meanwhile, it inhibits blood vessels development of the CAM of the embryo. On the other hand, we showed that this effect is due to the deregulation of several key controller genes of cell proliferation, survival, cell death and angiogenesis in several organs and tissues from exposed embryos.

EXPERIMENTAL DETAILS

Synthesis of 2D-MXene Nanosheets

$Ti_3C_2T_x$ sheets were prepared by the chemical removal of Al from Ti_3AlC_2 (MAX phase) using 48% HF solution [9]. Every 1 gm of Ti_3AlC_2 powder was chemically etched using 10 mL 48% HF solution and stirred for 18 hours at room temperature. The obtained etched MAX was washed, dried under vacuum, and intercalated with DMSO for 24 hours. Finally, the delamination step was performed using ultra-sonication under argon gas to get the desired delaminated MXene.

Characterization of MXene

The surface morphology and the elemental composition of the as-prepared MXene was determined using scanning electron microscopy (SEM) coupled with energy dispersive spectrometer (EDS). FEI Nova NanoSEM 450 was used to investigate the morphology of the synthesized MXenes. We examined the morphology of the as-prepared MXene sheets using Talos Transmission Electron Microscope (FEI), operated at 200 KV and provided with a new Ceta 16M camera. X-ray diffraction (XRD) was applied to study the crystal phase of the particle as prepared alkylated MXene using PAN analytical X-ray diffractometer equipped with a Cu-Kα1 radiation source ($\lambda = 1.5405$ Å).

Evaluation of the Effect of MXene Treatment on the Embryo

Fertilized chicken (White Leghorn) eggs were purchased from the Arab Qatari for Poultry Production and placed in an egg incubator at 37 °C with 70% humidity. Thirty eggs were used for each set of experiment. Embryos were treated with MXene suspension at day 3 of incubation, as described previously by our group [29]. Every embryo was treated with 30 μg of MXene in PBS suspension by traversing the amniotic membrane of the embryos using a microcapillary tube. PBS treated (30 μl) embryos were used as controls. Embryos were sacrificed at day 8 and autopsied; then, embryos as well as brain, liver and heart tissues were harvested for macroscopic examination and RNA extraction for RT-PCR analysis. Three independent sets of experiments were performed to induce reproducible results.

Chorioallantoic Membrane (CAM) Assay

Embryos at 5 days of incubation were used to explore the outcome MXene on the CAM. The CAM of the embryos were treated with 30 μg of the as-prepared MXene suspension which was placed on a circular glass cover slip as previously illustrated by our group [28]. PBS treated (30 μl) embryos were used as controls. After 24 h, the vascular development of the CAM was examined daily over the period of four days with a stereomicroscope, images were captured, and the number of branching points and length of the vessels were quantified using ImageJ software [30]. Three independent sets of experiments were performed to get reproducible results.

RNA Isolation and Reverse Transcription (RT)-PCR Analysis

Total RNA was purified from brain, heart and liver tissues of chicken embryos using the RNeasy Plus Mini Kit (Qiagen, Valencia, CA) according to the manufacturer's instructions. cDNA synthesis and PCR amplification were performed using Invitrogen Superscript III One-Step RT-PCR System with Platinum™ *Taq* DNA Polymerase Enzyme (ThermoFisher Scientific, USA) according to

Table I. Primer sets used for RT-PCR amplification.

Gene name	Primers
ATF-3 (Activating transcription factor-3)	5′-AAAAGCGAAGAAGGGAAAGG-3′
	5′-ATACAGGTGGGCCTGTGAAG-3′
FOXA-2 (Forkhead box A2)	5′-GACCTCTTCCCCTTCTACCG-3′
	5′-AGGTAGCAGCCGTTCTCAAA-3′
INHIB-A (Inhibin beta-A)	5′-GCCACCAAGAAACTCCATGT-3′
	5′-GCAACGTTTTCTTGGGTGTT-3′
MAPRE-2 (Microtubule-associated protein, RP/EB family, member 2)	5′-CAAAGGAGCCTTCCACAGAG-3′
	5′-GTCACTTCTGATGGCAGCAA-3′
RIPK-1 (Receptor (TNFRSF)-interacting serine-threonine kinase-1)	5′-CCGTACAGAATTGCAGCAGA-3′
	5′-TTCCATTAGCACACGAGCTG-3′
SERPINA-4 (Serpin peptidase inhibitor 4)	5′-CCAGCAAAAGGGAAAATGAA-3′
	5′-CACCACTGATGCCAGAGAGA-3′
VEGF-C (Vascular endothelial growth factor C)	5′-AGGGAACACTCCAGCTCTGA-3′
	5′-CTCCAAACTCTTTCCCCACA-3′
GAPDH (Glyceraldehyde-3-phosphate dehydrogenase)	5′-CCTCTCTGGCAAAGTCCAAG-3′
	5′-CATCTGCCCATTTGATGTTG-3′

the manufacturer's protocol. RT-PCR amplification was performed using primer sets for activating transcription factor-3 (ATF-3), forkhead box-A2 (FOXA2), inhibin beta-A (INHIBA), microtubule-associated protein RP/EB family member-2 (MAPRE-2), receptor (TNFRSF)-interacting serine-threonine kinase-1 (RIPK-1), serpin peptidase inhibitor-4 (SERPINA-4), vascular endothelial growth factor-C (VEGF-C) (Table I). GAPDH primers were used as an internal control.

In order to obtain a relative quantification of gene expressions, images acquired from RT-PCR were analyzed using ImageJ software 1.52 k [30]. The intensity of the bands relative to the GAPDH bands were used to calculate a relative expression of genes in each tissue (brain, heart and liver).

Statistical Analysis

Statistical significance was calculated for each of the three measurements. SPSS 64-bit version 23 was applied to carry out the previous tests where probabilities less than 0.05 ($p < 0.05$) were considered statistically significant.

RESULTS

Characterization of Ti_3C_2 MXene

MXene ($Ti_3C_2T_x$) was prepared as described in the methods section. Figure 1 shows the morphological features of the MXene powder. SEM images show the well-exfoliated MXene flakes (Fig. 1(A)). The as-synthesized MXene nanosheets are well delaminated with an average length of 650 nm and an average width of 450 nm as displayed by the TEM image in Figure 1(B).

Elemental analysis was conducted by Energy dispersive spectrometer (EDS) coupled in the SEM machine to determine the elemental composition in the synthesized MXene (Fig. 1(C)). XRD pattern of synthesized Mxene nanosheets (Fig. 1(D)) indicates the good etching of MAX phase to MXene due to the absence of the characteristic peak for Aluminum at $2\theta \sim 39°$ [31]. Furthermore, the presence of (110) peak at $\sim 61°$ 2θ in the XRD pattern of c-$Ti_3C_2T_x$ indicates less ordered arrangement of MXene flakes.

Effect of MXene on the Early Stage of the Normal Development of the Embryo

In order to explore the potential toxicity of MXene on the early stage of embryogenesis, we examined the effect of the MXene on chicken embryos on the 3rd day of incubation as described in the method section. We deposited 30 μg of MXene on 52 chicken embryos; in parallel, we treated 14 embryos with 30 μl of PBS in the same site as controls. Then, we examined the embryos every day for the next 5 days; we found that 24 ($\sim$46) of 52 embryos die before 8 days ($P < 0.05$) of incubation (Table II); while, only 1 embryo out of 14 controls ($\sim$7%) was found dead at the same period. The number of embryos that died during the subsequent period of MXene-treatment were 4, 3, 1 and 1 on days 2, 3, 4 and 5 of incubation, respectively, after exposure. The few live embryos which remained on day 5 after exposure were euthanized and dissected to isolate internal organs such as brain, heart and liver for further analysis.

Macroscopic and microscopic examination of embryos and organs were performed. We did not observe any considerable difference between MXene treated embryos and controls in terms of body size and shape in addition to internal organs (data not shown). However, the blood vessel development in some internal organs, such as liver, brain and heart are slightly inhibited in MXene-exposed embryos at 3 days of incubation (data not shown).

Effect of MXene ($Ti_3C_2T_x$) on Angiogenesis of the CAM Model

The effect of MXene on angiogenesis was assessed using the CAM of the chicken embryo at 5 days of

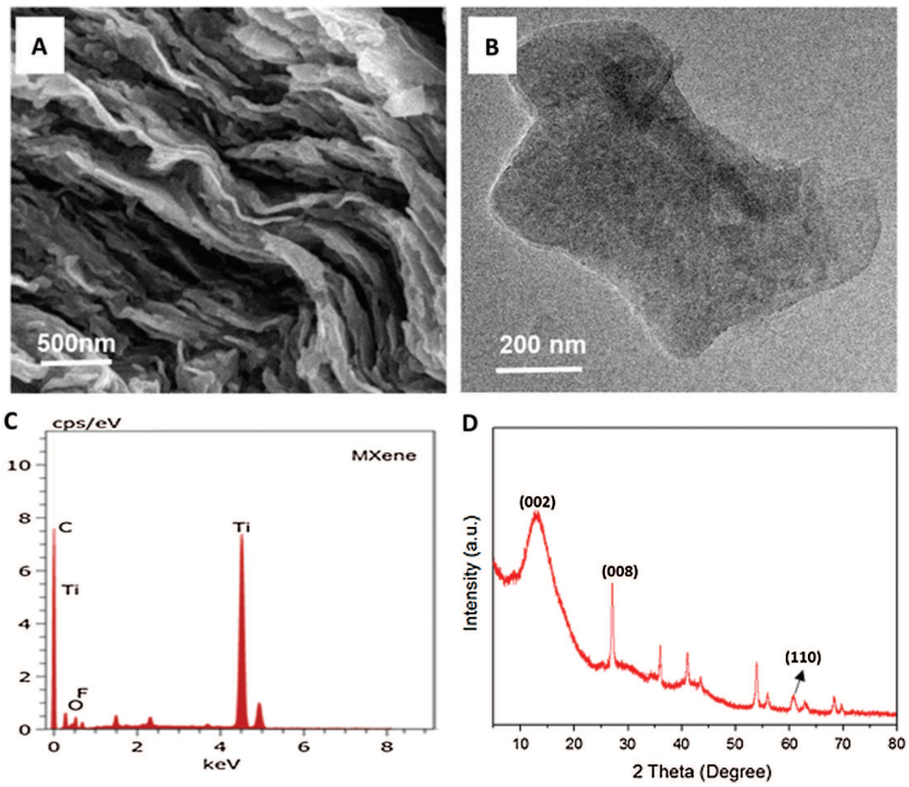

Figure 1. **Morphology of $Ti_3C_2T_x$ by SEM (A) and TEM analysis (B). EDS (C) and XRD pattern (D) of synthesized MXene.**

incubation as illustrated in the methods section. Significantly higher number of deaths was observed in MXene-exposed embryos 24 out of 34. While, 35% (12/34) of MXene-treated embryos died within 24 hours, 9% (2/22) of them died after 48 hours of exposure. More significantly, we found that MXene-treatment inhibited the formation of new blood vessels of the CAM compared to PBS treated controls (Figs. 2(A and B)). Quantitative analysis of obtained results indicates that the number of blood vessel junctions (measure of the newly formed blood vessels) was significantly less ($P < 0.0130$) for MXene-treated embryos compared to controls 81.05% reduction (Fig. 2(C)). Similarly, total length of blood vessels was also significantly less ($P < 0.0001$) for MXene treated embryos compared to controls, 54.45% reduction (Fig. 2(D)).

Table II. **Outcome of MXene ($Ti_3C_2T_x$) exposure on chicken embryos.**

Number of embryos*	Number of cases	Number of embryos dead before 9 days of incubation (%)
MXene-exposed	52	24 (46.15)
Control	14	1 (6.66)

Note: *Embryos were exposed at the 3rd day of incubation.

Outcome of MXene ($Ti_3C_2T_x$) on Gene Expression of Brain, Heart and Liver Tissues of Exposed Embryo

We examined the expression of ATF-3, FOXA-2, INHIBA, MAPRE2, RIPK-1, SERPINA-4 and VEGFC genes in brain, heart and liver tissues from MXene-treated and their matched control embryos using RT-PCR methodology. These genes were selected based on our previous investigations regarding the outcome of single walled carbon nanotubes (SWCNs) on the embryo and human normal bronchial epithelial cells, particularly in relation to their role as key regulators of cell proliferation, survival, cell death and angiogenesis [29, 32]. We found that ATF-3, FOXA-2, INHIBA, MAPRE2 and RIPK-1 genes are up-regulated in brain, heart and liver tissues of MXene-treated embryos in comparison with control tissues (Figs. 3 and 4); while, SERPINA-4 and VEGF-C genes are down-regulated in tissues from MXene-exposed embryo.

DISCUSSION

To the best of our knowledge, the effect of MXene ($Ti_3C_2T_x$) has not been sufficiently studied in conjunction with human health; however, few *in vitro* and *in vivo* studies have explored the effect of MXene nanosheets on biological systems [26, 33, 34]. While the effect of MXene during the early stage of vertebrate embryonic

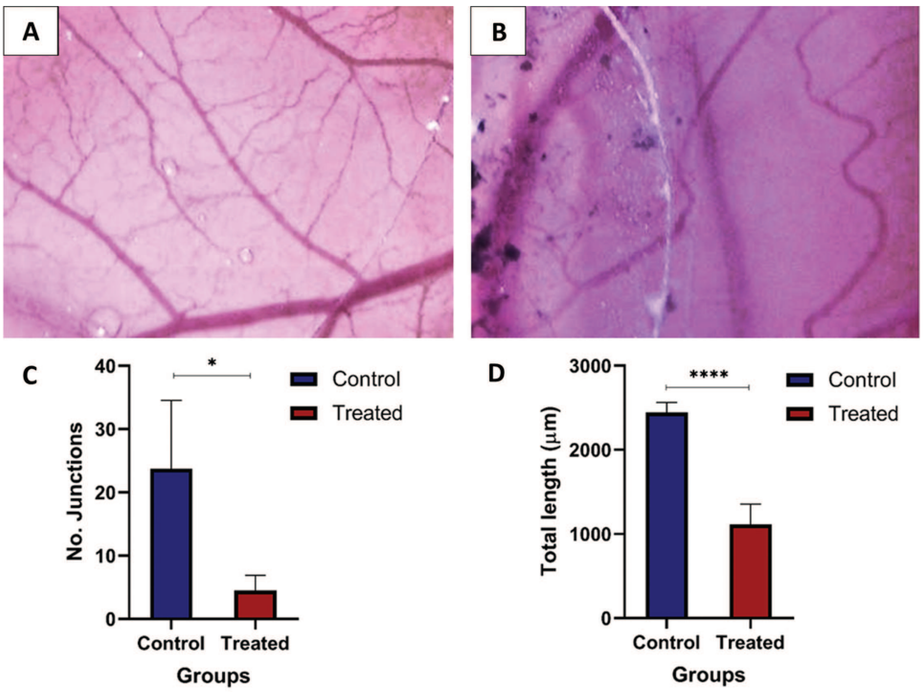

Figure 2. **Effect of MXene on angiogenesis of the chorioallantoic membrane (CAM) of the chicken embryo after 24 h of treatment (A). MXene treatment inhibits angiogenesis in comparison with the control (B). Number of junctions in controls versus MXene exposed embryos (C). Total length of blood vessels of controls versus MXene exposed embryos (D).**

development is still nascent; we herein report, for the first time, that MXene has a significant toxic effect on the early stages of embryogenesis and can inhibit angiogenesis of the CAM; in our study we used the chicken embryo model which is considered as an excellent experimental model for embryogenesis and angiogenesis [28, 29]. Our study pointed out that MXene has an important embryotoxic effect during normal development since ~46% of

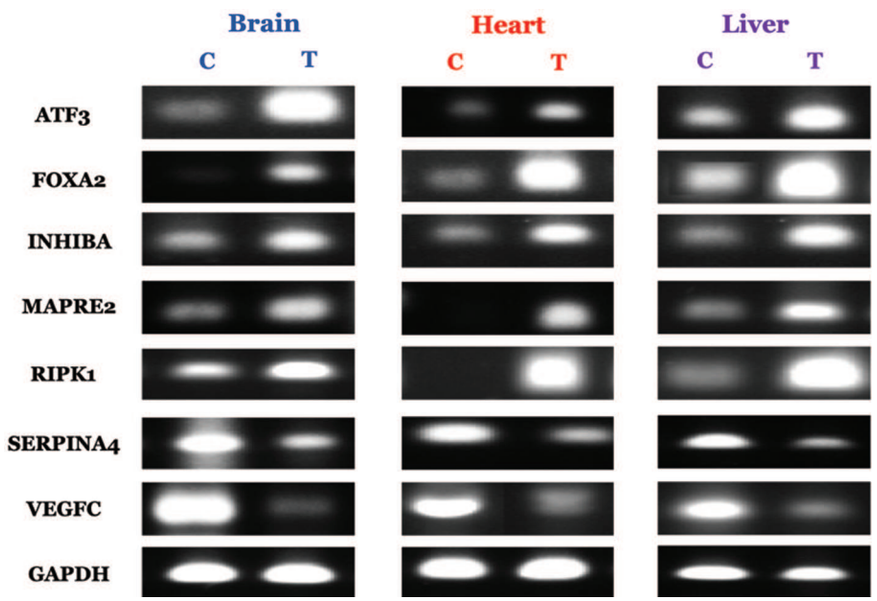

Figure 3. **RT-PCR analysis of ATF-3, FOXA-2, INHIBA, MAPRE2, RIPK-1, SERPINA-4 and VEGFC genes in brain, heart and liver tissues from normal and MXene-exposed embryos. This analysis was performed using normal tissue and their corresponding MXene-tissues from exposed embryo (C: Control tissues; T: MXene-exposed tissue). GAPDH gene amplified from the same tissue samples indicates similar loading in each group.**

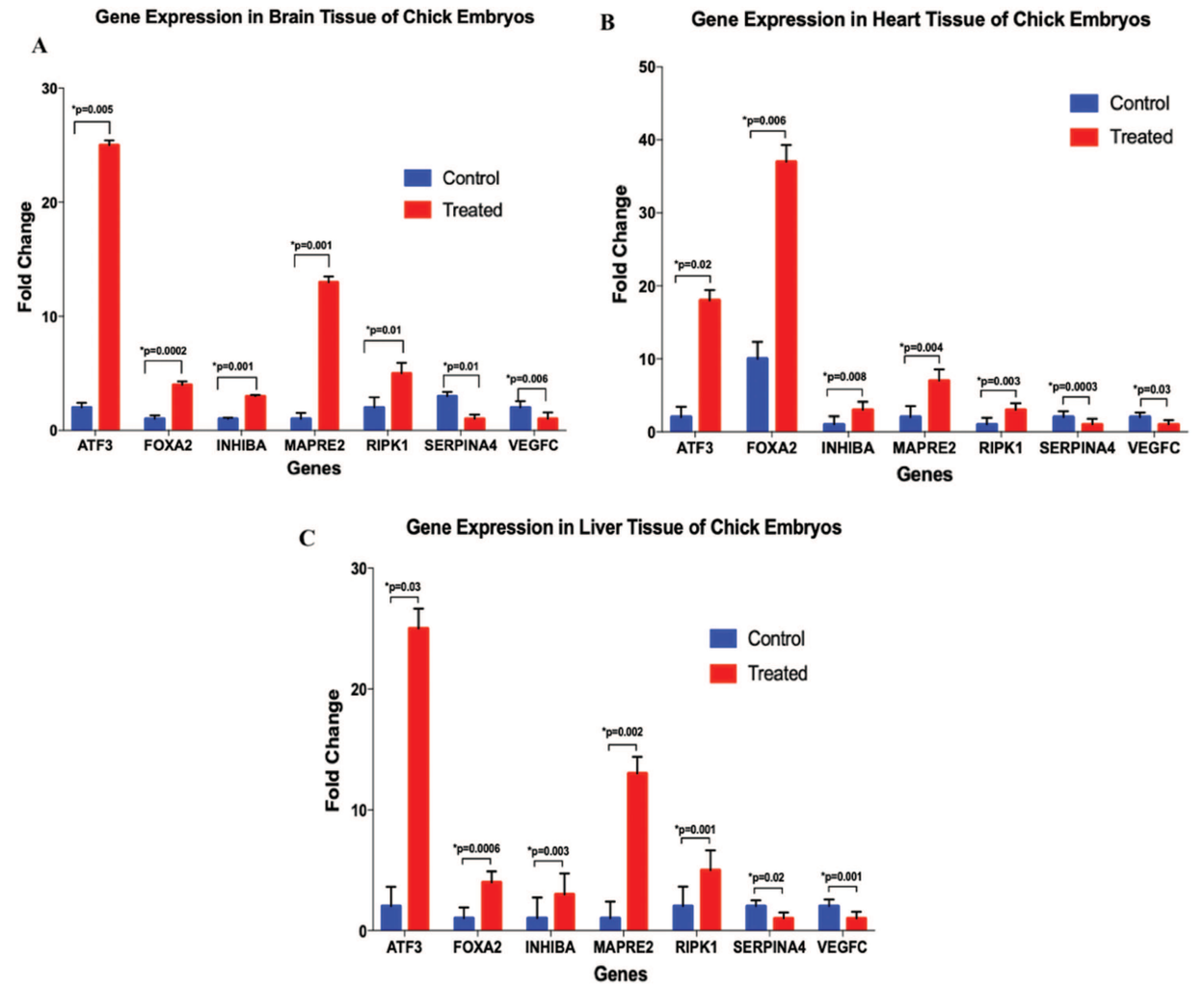

Figure 4. **Quantification of ATF-3, FOXA-2, INHIBA, MAPRE2, RIPK-1, SERPINA-4 and VEGFC gene expression of brain, heart and liver of MXene exposed embryos and their controls. We clearly note that ATF-3, FOXA-2, INHIBA, MAPRE2, RIPK-1, SERPINA-4 genes are up regulated in tissues from MXene-exposed embryos in comparison with their matched control tissues.**

MXene-treated embryos died within 1 to 5 days after exposure. Nevertheless, macroscopic analysis of embryos and organs did not display notable deviation from control groups in size or morphology. Meanwhile, we noted that MXene inhibits angiogenesis of the embryo and the CAM upon exposure at 5 days of incubation. While, earlier studies indicated that MXene treatment can induce oxidative stress and increase intracellular reactive oxygen species level in mammalian cells [22]. Therefore, we assumed that oxidative stress generated by MXene nanosheets might have resulted in toxicity and consequently mortality of exposed embryos. On the other hand, it has been recently demonstrated that MXene might induce higher toxicity towards human cancerous cell lines in comparison to normal ones [35]; meanwhile, a new study revealed that MXene has a limited toxic effect on zebrafish embryo [27]. Accordingly, we believe that different experimental models, such as mammalian and others, are needed to elucidate the actual effect and mechanism of MXene during the normal development of the embryo. Meanwhile, it is important to highlight that our present study reveals, for the first time, that MXene nanosheets can inhibit angiogenesis in different organs of exposed embryos and the CAM model. Several investigations explored the outcome of various nanomaterials *in vitro* and *in vivo* including angiogenesis [36–40]. Earlier studies reported the pro-angiogenic effect of various nanomaterials; however, other investigations showed some anti-angiogenic effect [41]. Several nanomaterials can act at molecular level and generate either favorable or adverse effects in a concentration dependent manner [42]. More specifically, previous reports pointed out that nanoparticles including single-walled carbon nanotubes (SWCNTs) can provoke apoptosis *in vitro* and embryotoxicity in addition to its ability to inhibit angiogenesis via the deregulation of several key controller genes related to cell proliferation, survival, cell death and

angiogenesis [29, 43]. Thus, in our present investigation we examined the effect of MXene on the expression patterns of a set of genes related to these important biological events. Accordingly, we studied the expression patterns of ATF3, FOXA2, INHBA, MAPRE2, RIPK2, SERPINA-4 and VEGF-C genes in brain, heart and liver tissues from MXene-exposed and their matched control embryos. We observed that ATF-3, FOXA-2, INHBA, MAPRE2 and RIPK-1 genes are up-regulated in MXene-treated embryonic tissues. On the other hand, it is essential to highlight that SERPINA-4 and VEGF-C genes are down-regulated in brain, heart and liver tissues of MXene-exposed embryos in comparison with their matched tissues from control embryos. Upregulation of FOXA2 is involved in the processes of proliferation, invasion and metastasis, as well as epithelial mesenchymal transition (EMT) [44], which are major events during embryogenesis and carcinogenesis. Similar to FOXA2, ATF3, MAPRE2 and RIPK1 are involved in controlling proliferation of cells; their over-expression results in uncontrolled cell growth [45, 46]. Furthermore, during normal development of the embryo, INHBA plays a key role in axis development and organogenesis [47]; higher expression is linked with toxic effects. On the other hand, SERPINA4 defends against vascular and organ injury and tumor progression; concordant with our data obtained, loss of SERPINA4 is associated with septic shock, hypertension, cardiovascular and renal injury and hepatic neoplasia in animal models [48]. VEGFC plays a role in development of blood vessels as well as lymphatic system; loss of VEGFC in *Xenopus laevis* tadpoles as well as zebrafish induces irregular blood vessel formation in addition to lymphatic vessel defects [49], which can induce toxicity in embryos.

These results are consistent with our previous studies concerning the outcome of SWCNTs on the early stage of the normal development and human normal bronchial epithelial cells [29, 32]. Thus, our present investigation clearly demonstrates that MXene may have potential toxic outcome on the early stages of embryogenesis which can be mediated by the deregulation of several genes including ATF3, FOXA2, INHBA, MAPRE2, RIPK2, SERPINA-4 and VEGF-C. However, further studies are required to conclusively verify the concentration dependent effect of MXene and other MXenes in chicken embryo as well as human health including the normal development of the embryo.

CONCLUSIONS

In this study, we used the chicken embryo model to explore the outcome of MXene exposure on the early stage of the embryo and angiogenesis. Our data pointed out, for the first time, that MXene at the studied concentration can provoke considerable adverse effect during embryogenesis and inhibit angiogenesis of the CAM. Accordingly, we found that at studied concentration, MXene deregulates a set of genes related to cell proliferation, survival, cell death and angiogenesis which are important biological events during normal development. However, the effect of lower concentrations of pure MXenes in addition to MXene based compounds on vertebrate embryos still need to be investigated. In addition, we believe that detailed *in vitro* and *in vivo* studies are still required to fully identify and generalize the outcome of MXene exposure and its mechanism of action in biological systems.

Acknowledgments: The authors would like to thank Mrs. Amal Kassab for her critical reading of the manuscript. We also acknowledge the support provided by the Central Laboratories Unit (CLU) of Qatar University. This work was supported by grants from Qatar University: QUHI-CMED-19/20-1 and GCC # 2017-002 QU/KU. The work of this paper was also partially supported by NPRP9-144-3-021 grant funded by Qatar National Research Fund (a part of Qatar Foundation). The statements made here are the sole responsibility of the authors.

REFERENCES

1. Augustine, R., Hasan, A., Nath, V.K.Y., Thomas, J., Augustine, A., Kalarikkal, N., Moustafa, A.-E.A. and Thomas, S., **2018**. Electrospun polyvinyl alcohol membranes incorporated with green synthesized silver nanoparticles for wound dressing applications. *Journal of Materials Science, Materials in Medicine, 29*(11), pp.163–163.
2. Augustine, R., Augustine, A., Kalarikkal, N. and Thomas, S., **2016**. Fabrication and characterization of biosilver nanoparticles loaded calcium pectinate nano-micro dual-porous antibacterial wound dressings. *Progress in Biomaterials, 5*(3–4), pp.223–235.
3. Augustine, R. and Hasan, A., **2020**. Emerging applications of biocompatible phytosynthesized metal/metal oxide nanoparticles in healthcare. *Journal of Drug Delivery Science and Technology*, p.101516.
4. Lu, S., Sui, L., Liu, J., Zhu, S., Chen, A., Jin, M. and Yang, B., **2017**. Near-infrared photoluminescent polymer-carbon nanodots with two-photon fluorescence. *Advanced Materials (Deerfield Beach, Fla.), 29*(15), DOI: 10.1002/adma.201603443.
5. Yang, Y., Wang, X., Liao, G., Liu, X., Chen, Q., Li, H., Lu, L., Zhao, P. and Yu, Z., **2018**. iRGD-decorated red shift emissive carbon nanodots for tumor targeting fluorescence imaging. *Journal of Colloid and Interface Science, 509*, pp.515–521.
6. Gao, S., Tang, G., Hua, D., Xiong, R., Han, J., Jiang, S., Zhang, Q. and Huang, C., **2019**. Stimuli-responsive bio-based polymeric systems and their applications. *Journal of Materials Chemistry B, 7*(5), pp.709–729.
7. Chimene, D., Alge, D.L. and Gaharwar, A.K., **2015**. Two-dimensional nanomaterials for biomedical applications: Emerging trends and future prospects. *Advanced Materials, 27*(45), pp.7261–7284.
8. Chatzistavrou, X., Newby, P. and Boccaccini, A.R., **2011**. 5-bioactive glass and glass-ceramic scaffolds for bone tissue engineering. *Bioactive Glasses*, edited by H. O. Ylänen, Woodhead Publishing. pp.107–128.
9. Naguib, M., Kurtoglu, M., Presser, V., Lu, J., Niu, J., Heon, M., Hultman, L., Gogotsi, Y. and Barsoum, M.W., **2011**. Two-dimensional nanocrystals produced by exfoliation of Ti_3AlC_2. *Advanced Materials, 23*(37), pp.4248–4253.

10. Fu, Z., Zhang, H., Si, C., Legut, D., Germann, T.C., Zhang, Q., Du, S., Francisco, J.S. and Zhang, R., **2018**. Mechanistic quantification of thermodynamic stability and mechanical strength for two-dimensional transition-metal carbides. *The Journal of Physical Chemistry C, 122*(8), pp.4710–4722.

11. Alhabeb, M., Maleski, K., Anasori, B., Lelyukh, P., Clark, L., Sin, S. and Gogotsi, Y., **2017**. Guidelines for synthesis and processing of two-dimensional titanium carbide ($Ti_3C_2T_x$ MXene). *Chemistry of Materials, 29*(18), pp.7633–7644.

12. Tian, Y., Que, W., Luo, Y., Yang, C., Yin, X. and Kong, L.B., **2019**. Surface nitrogen-modified 2D titanium carbide (MXene) with high energy density for aqueous supercapacitor applications. *Journal of Materials Chemistry A, 7*(10), pp.5416–5425.

13. Xiong, D., Li, X., Bai, Z. and Lu, S., **2018**. Recent advances in layered $Ti_3C_2T_x$ MXene for electrochemical energy storage. *Small, 14*(17), p.1703419.

14. Zhang, C., Ma, Y., Zhang, X., Abdolhosseinzadeh, S., Sheng, H., Lan, W., Pakdel, A., Heier, J. and Nüesch, F., **2020**. Two-dimensional transition metal carbides and nitrides (MXenes): Synthesis, properties, and electrochemical energy storage applications. *Energy & Environmental Materials,* pp.1–27.

15. Zhang, X., Zhang, Z. and Zhou, Z., **2018**. MXene-based materials for electrochemical energy storage. *Journal of Energy Chemistry, 27*(1), pp.73–85.

16. Naguib, M., Mochalin, V.N., Barsoum, M.W. and Gogotsi, Y., **2014**. 25th anniversary article: MXenes: A new family of two-dimensional materials. *Advanced Materials, 26*(7), pp.992–1005.

17. Chen, Q., Yang, Y., Lin, X., Ma, W., Chen, G., Li, W., Wang, X. and Yu, Z., **2018**. Platinum (iv) prodrugs with long lipid chains for drug delivery and overcoming cisplatin resistance. *Chemical Communications (Cambridge, England), 54*(42), pp.5369–5372.

18. Yu, M., Su, D., Yang, Y., Qin, L., Hu, C., Liu, R., Zhou, Y., Yang, C., Yang, X., Wang, G. and Gao, H., **2019**. D-T7 peptide-modified pegylated bilirubin nanoparticles loaded with cediranib and paclitaxel for antiangiogenesis and chemotherapy of glioma. *ACS Applied Materials & Interfaces, 11*(1), pp.176–186.

19. Yu, Y., Xu, Q., He, S., Xiong, H., Zhang, Q., Xu, W., Ricotta, V., Bai, L., Zhang, Q., Yu, Z., Ding, J., Xiao, H. and Zhou, D., **2019**. Recent advances in delivery of photosensitive metal-based drugs. *Coordination Chemistry Reviews, 387*, pp.154–179.

20. Yang, K., Feng, L., Shi, X. and Liu, Z., **2013**. Nano-graphene in biomedicine: Theranostic applications. *Chemical Society Reviews, 42*(2), pp.530–547.

21. Lin, H., Gao, S., Dai, C., Chen, Y. and Shi, J., **2017**. A two-dimensional biodegradable niobium carbide (MXene) for photothermal tumor eradication in NIR-I and NIR-II biowindows. *Journal of the American Chemical Society, 139*(45), pp.16235–16247.

22. Jastrzębska, A.M., Szuplewska, A., Wojciechowski, T., Chudy, M., Ziemkowska, W., Chlubny, L., Rozmysłowska, A. and Olszyna, A., **2017**. In vitro studies on cytotoxicity of delaminated Ti_3C_2 MXene. *Journal of Hazardous Materials, 339*, pp.1–8.

23. Dai, C., Chen, Y., Jing, X., Xiang, L., Yang, D., Lin, H., Liu, Z., Han, X. and Wu, R., **2017**. Two-dimensional tantalum carbide (MXenes) composite nanosheets for multiple imaging-guided photothermal tumor ablation. *ACS Nano, 11*(12), pp.12696–12712.

24. Lin, H., Chen, Y. and Shi, J., **2018**. Insights into 2D MXenes for versatile biomedical applications: Current advances and challenges ahead. *Advanced Science, 5*(10), p.1800518.

25. Liu, Z., Zhao, M., Lin, H., Dai, C., Ren, C., Zhang, S., Peng, W. and Chen, Y., **2018**. 2D magnetic titanium carbide MXene for cancer theranostics. *Journal of Materials Chemistry B, 6*(21), pp.3541–3548.

26. Nasrallah, G.K., Al-Asmakh, M., Rasool, K. and Mahmoud, K.A., **2018**. Ecotoxicological assessment of $Ti_3C_2T_x$ (MXene) using a zebrafish embryo model. *Environmental Science: Nano, 5*(4), pp.1002–1011.

27. Hussein, E.A., Zagho, M.M., Rizeq, B.R., Younes, N.N., Pintus, G., Mahmoud, K.A., Nasrallah, G.K. and Elzatahry, A.A., **2019**. Plasmonic MXene-based nanocomposites exhibiting photothermal therapeutic effects with lower acute toxicity than pure MXene. *International Journal of Nanomedicine, 14*, pp.4529–4539.

28. Augustine, R., Alhussain, H., Hasan, A., Ahmed, M.B., Yalcin, H.C. and Al-Moustafa, A.E., **2019**. A novel in ovo model to study cancer metastasis using chicken embryos and GFP expressing cancer cells. *BJBMS, 20*(1), pp.140–148.

29. Roman, D., Yasmeen, A., Mireuta, M., Stiharu, I. and Al Moustafa, A.-E., **2013**. Significant toxic role for single-walled carbon nanotubes during normal embryogenesis. *Nanomedicine: Nanotechnology, Biology and Medicine, 9*(7), pp.945–950.

30. Schneider, C.A., Rasband, W.S. and Eliceiri, K.W., **2012**. NIH image to imageJ: 25 years of image analysis. *Nature Methods, 9*(7), pp.671–675.

31. Raagulan, K., Braveenth, R., Kim, B.M., Lim, K.J., Lee, S.B., Kim, M. and Chai, K.Y., **2020**. An effective utilization of MXene and its effect on electromagnetic interference shielding: Flexible, free-standing and thermally conductive composite from MXene–PAT–poly(*p*-aminophenol)–polyaniline co-polymer. *RSC Advances, 10*(3), pp.1613–1633.

32. Alazzam, A., Mfoumou, E., Stiharu, I., Kassab, A., Darnel, A., Yasmeen, A., Sivakumar, N., Bhat, R. and Al Moustafa, A.E., **2010**. Identification of deregulated genes by single wall carbon-nanotubes in human normal bronchial epithelial cells. *Nanomedicine, 6*(4), pp.563–569.

33. Rafieerad, A., Yan, W., Sequiera, G.L., Sareen, N., Abu-El-Rub, E., Moudgil, M. and Dhingra, S., **2019**. Application of Ti_3C_2 MXene quantum dots for immunomodulation and regenerative medicine. *Advanced Healthcare Materials, 8*(16), p.1900569.

34. Soleymaniha, M., Shahbazi, M.-A., Rafieerad, A. R., Maleki, A. and Amiri, A., **2019**. Promoting role of MXene nanosheets in biomedical sciences: Therapeutic and biosensing innovations. *Advanced Healthcare Materials, 8*(1), p.1801137.

35. Szuplewska, A., Rozmysłowska-Wojciechowska, A., Poźniak, S., Wojciechowski, T., Birowska, M., Popielski, M., Chudy, M., Ziemkowska, W., Chlubny, L., Moszczyńska, D., Olszyna, A., Majewski, J.A. and Jastrzębska, A.M., **2019**. Multilayered stable 2D nano-sheets of Ti_2NT_x MXene: Synthesis, characterization, and anticancer activity. *Journal of Nanobiotechnology, 17*(1), p.114.

36. Barui, A.K., Veeriah, V., Mukherjee, S., Manna, J., Patel, A.K., Patra, S., Pal, K., Murali, S., Rana, R.K., Chatterjee, S. and Patra, C.R., **2012**. Zinc oxide nanoflowers make new blood vessels. *Nanoscale, 4*(24), pp.7861–7869.

37. Augustine, R., Dalvi, Y.B., Nath, V.K.Y., Varghese, R., Raghuveeran, V., Hasan, A., Thomas, S. and Sandhyarani, N., **2019**. Yttrium oxide nanoparticle loaded scaffolds with enhanced cell adhesion and vascularization for tissue engineering applications. *Materials Science and Engineering: C, 103*, p.109801.

38. Augustine, R., Hasan, A., Patan, N.K., Augustine, A., Dalvi, Y.B., Varghese, R., Unni, R.N., Kalarikkal, N., Al Moustafa, A.-E. and Thomas, S., **2019**. Titanium nanorods loaded PCL meshes with enhanced blood vessel formation and cell migration for wound dressing applications. *Macromolecular Bioscience, 19*(7), p.1900058.

39. Das, S., Singh, S., Dowding, J.M., Oommen, S., Kumar, A., Sayle, T.X.T., Saraf, S., Patra, C.R., Vlahakis, N.E., Sayle, D.C., Self, W.T. and Seal, S., **2012**. The induction of angiogenesis by cerium oxide nanoparticles through the modulation of oxygen in intracellular environments. *Biomaterials, 33*(31), pp.7746–7755.

40. Augustine, R., Dan, P., Sosnik, A., Kalarikkal, N., Tran, N., Vincent, B., Thomas, S., Menu, P. and Rouxel, D., **2017**. Electrospun poly(vinylidene fluoride-trifluoroethylene)/zinc oxide nanocomposite tissue engineering scaffolds with enhanced cell adhesion and blood vessel formation. *Nano Research, 10*(10), pp.3358–3376.

41. Roma-Rodrigues, C., Heuer-Jungemann, A., Fernandes, A.R., Kanaras, A.G. and Baptista, P.V., **2016**. Peptide-coated gold nanoparticles for modulation of angiogenesis in vivo. *International Journal of Nanomedicine, 11*, pp.2633–2639.

42. Augustine, R., Mathew, A.P. and Sosnik, A., **2017**. Metal oxide nanoparticles as versatile therapeutic agents modulating cell signaling pathways: Linking nanotechnology with molecular medicine. *Applied Materials Today, 7*, pp.91–103.

43. Al Moustafa, A.-E., Mfoumou, E., Roman, D.E., Nerguizian, V., Alazzam, A., Stiharu, I. and Yasmeen, A., **2016**. Impact of single-walled carbon nanotubes on the embryo: A brief review. *International Journal of Nanomedicine, 11*, pp.349–355.

44. Wang, B., Liu, G., Ding, L., Zhao, J. and Lu, Y., **2018**. FOXA2 promotes the proliferation, migration and invasion, and epithelial mesenchymal transition in colon cancer. *Experimental and Therapeutic Medicine, 16*(1), pp.133–140.

45. Perez, S., Vial, E., van Dam, H. and Castellazzi, M., **2001**. Transcription factor ATF3 partially transforms chick embryo fibroblasts by promoting growth factor-independent proliferation. *Oncogene, 20*(9), pp.1135–1141.

46. Rickard, J.A., O'Donnell, J.A., Evans, J.M., Lalaoui, N., Poh, A.R., Rogers, T., Vince, J.E., Lawlor, K.E., Ninnis, R.L., Anderton, H., Hall, C., Spall, S.K., Phesse, T.J., Abud, H.E., Cengia, L.H., Corbin, J., Mifsud, S., Di Rago, L., Metcalf, D., Ernst, M., Dewson, G., Roberts, A.W., Alexander, W.S., Murphy, J.M., Ekert, P.G., Masters, S.L., Vaux, D.L., Croker, B.A., Gerlic, M. and Silke, J., **2014**. RIPK1 regulates RIPK3-MLKL-driven systemic inflammation and emergency hematopoiesis. *Cell, 157*(5), pp.1175–1188.

47. Gurdon, J.B., Harger, P., Mitchell, A. and Lemaire, P., **1994**. Activin signalling and response to a morphogen gradient. *Nature, 371*(6497), pp.487–492.

48. Chao, J., Bledsoe, G. and Chao, L., **2016**. Protective role of kallistatin in vascular and organ injury. *Hypertension (Dallas, Tex.: 1979), 68*(3), pp.533–541.

49. Küchler, A.M., Gjini, E., Peterson-Maduro, J., Cancilla, B., Wolburg, H. and Schulte-Merker, S., **2006**. Development of the zebrafish lymphatic system requires vegfc signaling. *Current Biology, 16*(12), pp.1244–1248.